

Removal of naphthalene from aqueous solutions by phosphorus doped-titanium dioxide coated on silica phosphoric acid under visible light

Bahman Banaei^a, Amir Hessam Hassani^{a,*}, Farhang Tirgir^{b,*}, Abdolmajid Fadaei^c, Seyed Mehdi Borghaei^d

^aDepartment of Environmental Engineering, Faculty of Natural Resources and Environment, Science and Research Branch, Islamic Azad University, Tehran, Iran, emails: ahhassani@sbiau.ac.ir (A.H. Hassani), Bahman_14929@yahoo.com (B. Banaei)

^bDepartment of Chemistry, Faculty of Sciences, Shahrekord Branch, Islamic Azad University, Shahrekord, Iran, email: Tirgir588@gmail.com

^cDepartment of Environmental Health Engineering, School of Health, Shahrekord University of Medical Sciences, Shahrekord, Iran, email: ali2fadae@yahoo.com

^dDepartment of Chemistry and Environment, Faculty of Chemistry and Oil Industry, Sharif University of Technology, Tehran, Iran, email: mborghei@sharif.edu

Received 29 June 2020; Accepted 12 February 2021

ABSTRACT

In this research, titanium dioxide-phosphorus (TiO₂-P) immobilized on silica phosphoric acid (SPA) was prepared by a simple modified sol-gel method with SPA as a precursor instead of phosphoric acid. TiO₂-P thin film photocatalyst immobilized on SPA as a novel high-efficiency photocatalyst was investigated to remove naphthalene as a toxic compound from wastewater. The novel resulting photocatalyst were characterized by energy-dispersive X-ray (EDX) and X-ray diffraction pattern revealed nano-photocatalyst TiO₂-P with the average size of 15–20 nm. EDX analysis showed the presence of phosphorus elements in the crystalline structure of TiO₂ and diffuse reflectance spectroscopy showed the energy bandgap narrowing and transfer of photocatalytic activity of TiO₂-P to the visible region. The excellent photocatalytic activity of TiO₂-P/SPA compared with TiO₂-N,S as thin films coated on glass microspheres. The results showed that the optimal pH, time, concentration, and efficiency removal of naphthalene for TiO₂-P were 5, 50 min, 25 mg/L, and 92.12% and TiO₂-N,S catalyst were 5, 60 min, 25 mg/L, and 88.47%, respectively ($P < 0.05$). The removal of chemical oxygen demand in pH 5 for TiO₂-N,S was obtained 79.26% and for TiO₂-P was obtained 81.64%. In this research, the ability to use immobilized TiO₂-P in SPA can be used as a new, effective and practical method in the treatment of water and industrial wastewater containing naphthalene in the presence of visible light.

Keywords: Naphthalene; Titanium dioxide-phosphorus; Silica phosphoric acid; Visible light; Titanium dioxide

1. Introduction

Hydrocarbons such as polycyclic aromatic hydrocarbons (PAHs) consist of two or more aromatic rings which fused together are the main constituents of the petroleum, dyes, plastics, and pesticides that are not biodegradable would remain in the environment for a long time, which

have side effects on human health and aquatic environment [1–3]. PAHs cause various cancers in the respiratory organs, including lung and laryngeal cancers, as well as cancers of the reproductive organs, including the scrotum, bladder, and prostate. These compounds are produced mainly from the incomplete combustion or pyrolysis of organic material including gas, oil, coal, petroleum, and wood [4,5].

* Corresponding author.

PAHs have recently drawn substantial attention in studies on water, soil, and air pollution because they are extremely mutagenic, carcinogenic, and teratogenic [6,7]. Naphthalene ($C_{10}H_8$) is the smallest PAH, consisting of two fused benzene rings and the main compound that has the most solubility in aqueous media [8,9].

Physical processes are not efficient for PAHs pollution because they are unable to degrade these contaminants [10,11]. Accordingly, chemical processes are the most effective methods to convert these substances. Out of the chemical processes, direct photolysis is one of the main transformation processes that are effective on the fate of PAHs in the aquatic environment [11]. These challenges have culminated in designing specific methods based on advanced oxidation processes (AOPs), that is, a modern technology for water and wastewater treatment [12]. AOPs act based on the production of unstable species with high reactivity tendency (e.g., H_2O_2 , $O_2^{\bullet-}$ and OH^{\bullet}) to convert the resistant organic compounds to the inert components [12].

TiO_2 one of the most semiconductors using for photocatalytic reactions. Therefore, TiO_2 photocatalysts doped with nonmetals increased photocatalytic performance in the visible light region [13].

In the anatase crystalline form, solid TiO_2 serves as a semiconductor that is able to promote an electron (e^-) from the valence band (VB) to the conduction band (CB) under ultraviolet irradiation, leaving a positive hole (h^+) at the site in which the electron has been originally captured. When TiO_2 suspends in water, both the electron and the hole can vary actively generate radicals (hydroxide and superoxide) in the oxidative degradation of organic pollution in water Eqs. (1)–(5), [8,14]. Mechanism of formation of superoxide and hydroxyl radicals in TiO_2 -catalyzed water by (EG = gap energy) is depicted in Fig. 1:

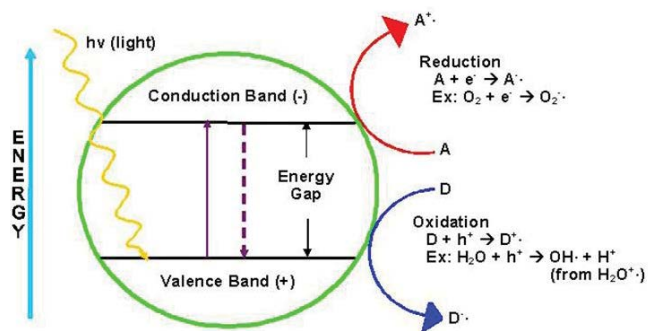
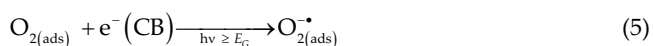
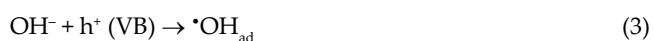
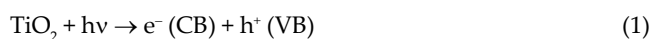


Fig. 1. Mechanism of formation of hydroxyl and superoxide radicals in water catalyzed by TiO_2 .

The literature about naphthalene oxidation by photocatalysis shows that degradation yields various compounds such as naphthols, naphthoquinones, and cinnamaldehydes and that naphthalene is finally completely mineralized into CO_2 and H_2O . Due to their eco-friendly nature and high optical activity, low price, low toxicity, high chemical and thermal stability, heterogeneous photocatalysts such as anatase TiO_2 crystals are regarded as the most popular photocatalysts [15–17]. Therefore, to modify this intrinsic property of TiO_2 and produce a new photocatalyst that is capable of keeping its photocatalytic activity in exposure to sunlight, methods such as doping with noble metals, metal ions, and anions (C, N, F, and S) are being developed [18–21]. Jafari et al. [22] doped N and S elements on the TiO_2 network to reduce the energy band gap and increase the optical activity of TiO_2 in a visible light region to remove naphthalene in an aqueous solution.

Doping phosphorus with TiO_2 makes the gap between two strips of capacity and conductivity narrower, and therefore leads to absorption in the visible region [23–25].

The efficiency of the oxidation techniques is dependent on different parameters, such as UV/visible-light intensity, the oxidant dose, free radical generation rate, reaction time, pH, initial concentration, and physico-chemical properties of the target pollutant, and the constituents of the water matrix (such as the presence of anions, suspended materials) [26–28]. In this study, in addition to the previous work, the new catalyst phosphorus doped-titanium dioxide [26] (TiO_2 -P) coated on silica phosphoric acid (SPA) was prepared and will be compared with the TiO_2 -N,S catalyst coated in glass microspheres to remove naphthalene from aqueous environments. SPA was synthesized according to previous literature [26], it was prepared by reaction of dry phosphoric acid with silica chloride. Using visible light that effect different parameters, such as the initial concentration of naphthalene, pH, radiation time, and COD. The TiO_2 -P/SPA were assayed by scanning electron microscopy (SEM) and energy-dispersive X-ray (EDX).

2. Materials and methods

2.1. Photocatalyst synthesis

All chemical materials were purchased from Germany's Merck Company. In order to immobilize the prepared sol of tetrabutyl titanate on a substrate, 500 microns in diameter glass microspheres made in Glass Beads were used. First, the glass microspheres were washed with a detergent solution and placed in dilute hydrochloric acid for 8 h and placed in an oven at $60^\circ C$ for 4 h to eliminate possible contamination and the glass microspheres for 30 min rinsed in the ultrasonic tub for minutes. TiO_2 -N,S nanocatalyst coated in glass bead was synthesized using sol-gel method according to previous literature [22]. TiO_2 -P coated on SPA glass microspheres was prepared through hydrolysis of tetrabutyl titanate in presence of SPA as the precursor of phosphor (P) instead of hypophosphorous acid. First, SPA was synthesized according to previous literature [26], it was prepared by reaction of dry phosphoric acid with silica chloride. For the preparation of silica chloride, thionyl chloride was reacted with dry silica gel.

The acidic capacity of SPA was determined via titration of 0.2 g of SPA with a standard solution of NaOH and calculated 10.62 mmol g⁻¹. P-doped TiO₂ Coated on SPA glass microspheres was prepared by a simple sol-gel method referring to that of P-doped TiO₂ reported by Lin et al. [28]. The atomic ratio of P to Ti in the precursors was 0.01. The typical synthesis procedure for P-doped TiO₂ is as follows: at first, 32.4 mg of SPA was dispersed in 100 mL of ethanol. The solution was stirred magnetically for 30 min, followed by the addition of 3.4 mL of tetrabutyl titanate. The mixture was stirred under anaerobic conditions (purged with N₂) for 2 h at room temperature, deionized water was then added dropwise to the vigorously stirring solution. The solution was aged at room temperature for 24 h and then stirred again at 90°C in a water bath to gelation, and dried at 100°C for about 8 h in air, to vaporize water and alcohol in the gels. The resulting product is ground into a fine powder and becomes a xerogel sample. The synthesized xerogel samples were calcinated at 600°C (as optimum temperature) for 3 h, to obtain TiO₂-P Coated on SPA glass microspheres (Fig. 2).

2.2. Study of photocatalyst properties

The crystallinity and particle size of the prepared TiO₂-P/SPA film on glass spheres were investigated by the X-ray diffraction (XRD) patterns collected in the range 20–80 (2θ) using a Philips CM120 (Netherlands) X'pert pro MPD device. The mean crystalline particle size of the anatase phase was estimated by Scherer equation [29]. The TiO₂-P photocatalytic band gap was obtained

using ultraviolet reflection spectroscopy (UV-vis) via the Shimadzu UV-1800 spectrophotometer [22].

2.3. Study of photocatalyst optical activity

Photocatalytic activities of TiO₂-P/SPA have been evaluated by measuring the photodegradation naphthalene solution under visible light irradiation. Fig. 3 shows the reactor used for the photocatalytic experiment according to previous work [22]. The degradation of naphthalene has been estimated by measuring the concentration of naphthalene at a defined time interval by using the UV-vis spectrophotometer at 276 nm [30]. Interestingly, naphthalene has a sharp absorption peak at 219 nm which this wavelength has no linear relationship between the amount of adsorption and concentration, so the wavelength of 276 for kinetic evaluation is used. The initial concentrations of naphthalene solution were chosen to be 5, 15, 25, 40, and 50 mg/L. The naphthalene solubility in water is a function of the solution temperature and its solubility is 31.6 mg/L at 25°C. The temperature of the reservoir containing naphthalene solution is 30°C. The interior temperature of the chamber about is 40°C due to the lamp heat. Different concentrations of naphthalene solution include 5, 15, and 25 mg/L were prepared in distilled water without organic solvent. In order to make naphthalene solution at concentrations of 40 and 50 mg/L, methanol solvent was used and prepared according to previous work [22]. Solutions were made for at least three replicates for each concentration and only one catalyst bed was used for each of the three replicates. After each use, the catalyst was washed more than a few times with distilled

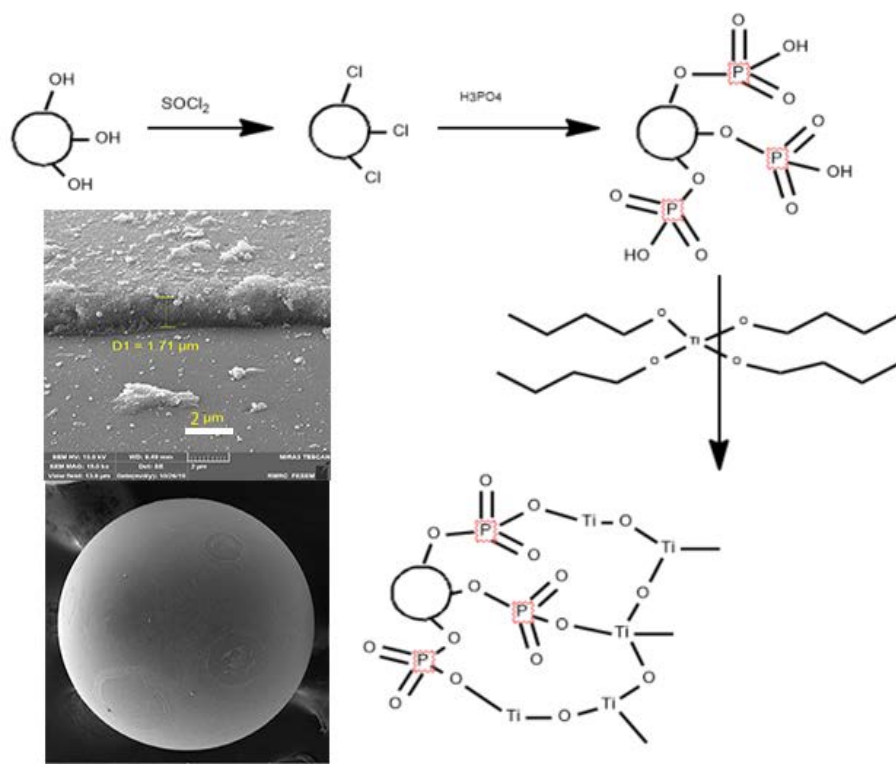


Fig. 2. Schematic diagram of TiO₂-P/SPA catalyst preparation.



Fig. 3. Schematic diagram of the pilot: (1) visible light, (2) mirror, (3) photoreactor, (4) TiO₂-P/SPA catalyst coated on glass microspheres, (5) reactor containing naphthalene solution, (6) condenser, (7) magnetic stirrer, (8) thermometer, and (9) cooler pump and cold water tank.

water, sonicated and dried at 100°C for 90 min and recycled. Initially, 500 mL of naphthalene solution with a constant concentration of 5 mg/L naphthalene was prepared at a temperature of 30°C and pHs of 3, 5, 7, and 9 were tested in the pilot of Fig. 3 according to previous work [22]. At each pH, the excitation has been carried out with a table lamp (visible light, output; 450 W) with 100 mL of 0.1 M aqueous solution of naphthalene and 18 g of the catalyst. The degradation of naphthalene is estimated by measuring the concentration of naphthalene over a specified period of time using a US-made UV-vis spectrophotometer (Perkin Elmer, Germany) at a maximum wavelength of 276 nm [22,30]. We first allowed the solutions of naphthalene were rotated at 20 min of darkness period before the visible light to get the adsorption–desorption equilibrium after which the initial concentration of naphthalene has been indicated as C_0 . To keep the temperature constant at 25°C inside the reactor, a cooler pump and a cold water tank connected to the valve was used. The degradation efficiency of naphthalene was calculated using the equivalent Eq. (6):

$$\eta = \frac{C_0 - C_t}{C_0} \times 100 \quad (6)$$

where C_0 is the initial concentration and C_t is the residual concentration of naphthalene after time t , and η is the naphthalene elimination percentage. All experiments were done in triplicate and the mean value was reported.

2.4. Chemical oxygen demand analysis

Samples were taken at different time intervals, the volume of any sample for COD measurement is 10 mL. The methodology is based on the oxidation of the organic carbon by potassium dichromate ($K_2Cr_2O_7$, 4N) in an acidic medium, thus conversion into carbon dioxide and water was done according to the standard method in the wastewater test [31].

2.5. Statistical analysis

One-way analysis of variance (ANOVA) was used to determine the accuracy of the test. In addition, Tukey's test was used to define p -value and the standard deviation.

3. Results and discussion

3.1. Morphological and structural properties of photocatalyst

In order to investigate elemental analysis and to calculate the weight percent and atomic percent of the elements existing on TiO₂-P nanocatalyst coated on SPA, EDX analysis was used. Figs. 4a and b illustrate EDX analysis of TiO₂-P thin film on SPA and Figs. 4c–e illustrate its corresponding SEM images. Fig. 4b shows the peaks of thin layer TiO₂-P coated on glass microspheres which confirm the presence of Ti and Si with the presence of P in the structure of the thin film of TiO₂. It should be noted that the elements of Mg, Na, and Ca in the EDX analysis spectrum are associated with the glass microspheres structure. Also, EDX analysis (Fig. 4b) shows the peaks related to the presence of P are at 0.5 keV and Ti at about 1.5–8.5 keV. According to Fig. 4b, elemental analysis of thin-film TiO₂-P coated on glass microspheres indicates 54.32 wt.% oxygen, 20.65 wt.% silicon, 6.10 wt.% sodium, 1.89 wt.% magnesium, 3.28 wt.% calcium (which is related to glass microspheres), 13.56 wt.% titanium, and phosphorus 0.21 wt.% representing that the new photocatalytic layer contains doped P atom. The SEM images of TiO₂-P thin film coated on SPA glass microspheres are shown in Figs. 4c. The thickness of TiO₂-P thin film which is equal to 1.73 μm compared (Figs. 4d) the thickness of this TiO₂-N,S thin film is equal to 693.68 nm according to previous literature [22]. Fig. 4e demonstrates the nano size of TiO₂-P particles in the thin film, which is evaluated to be 10–20 nm. TiO₂-P thin film coated on SPA glass microspheres has more thickness film than TiO₂-N,S which is equal to 693.68 nm [22],

because the phosphorus atoms were the covalent band with a hydroxyl group in the surface of glass microspheres. The hydroxyl group of phosphoric acid on the surface of the glass microspheres is good interaction with the prepared sol of tetrabutyl titanate via hydrogen bonding.

The crystal structure of the catalyst was investigated by XRD, phase composition, and particle size of TiO_2 -P as a thin film coated on SPA glass microspheres and the effect of phosphorus doping on particle size and crystal phase. Fig. 5 shows the XRD patterns of TiO_2 -P thin film coated on SPA glass microspheres. It is clear from Fig. 5

that the TiO_2 -P sample is present in an anatase phase, which is shown with the appearance of a diffraction peak of about 25.5° (JCPDS file number = 01-089-4921). Recently, Yingying et al. [32] have observed the absorption blue shift for their phosphorus-doped TiO_2 sample whereas Lin et al. [25] have observed absorption redshift for their phosphorus-doped samples. Yang et al. [35] reported the reduction of the anatase TiO_2 bandgap in the calculations of the electronic structure of TiO_2 because of the presence of doped phosphorus due to the replacement of pentavalent phosphorus (P^{5+}) to Ti^{4+} sites.

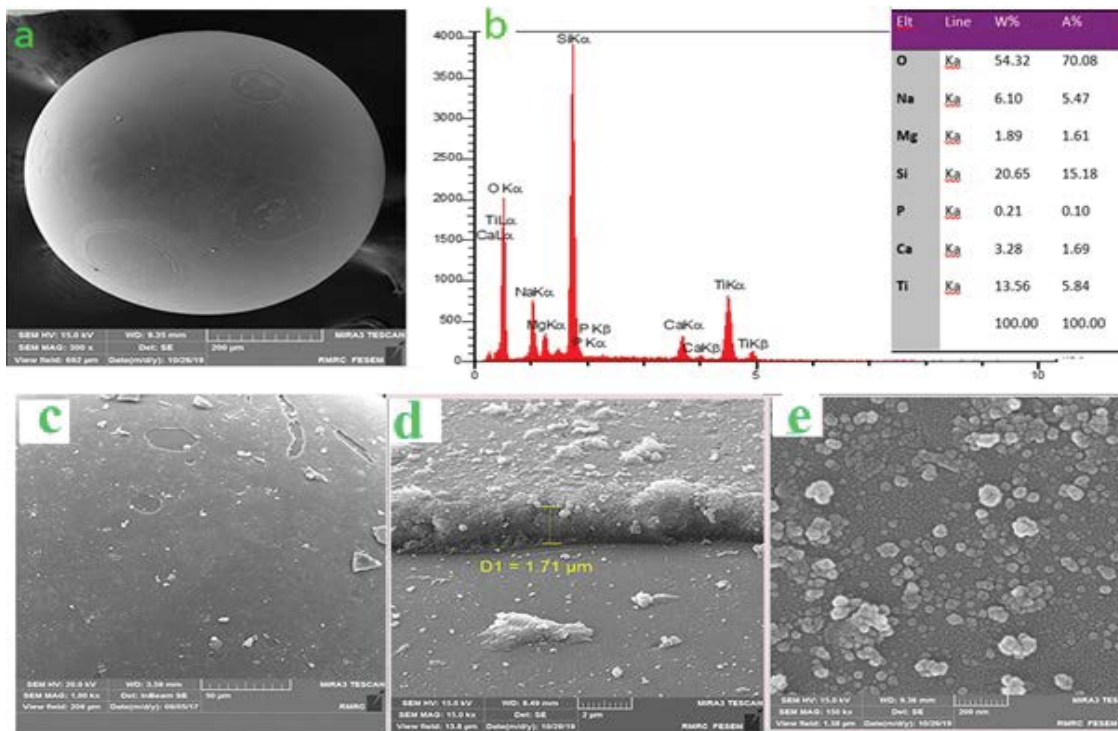


Fig. 4. EDX spectrum and SEM images related to TiO_2 -P coated on SPA, respectively: (a) SEM image of SPA glass microspheres which coated with TiO_2 -P thin film, (b) EDX analysis related to TiO_2 -P coated on SPA glass microspheres, (c) SEM image of uniform TiO_2 -P thin film coated on the SPA surface, (d) thickness of TiO_2 -P thin film which is equal to $1.73 \mu m$, and (e) high-resolution image of nanometer-sized TiO_2 -P particles on the SPA glass microspheres surface.

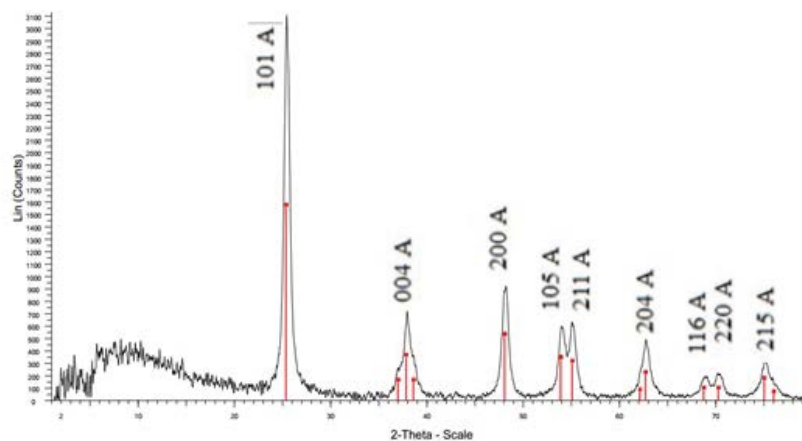


Fig. 5. XRD pattern of TiO_2 -P thin film doped on SPA glass microspheres.

UV-vis diffuse reflection spectroscopy (DRS) analysis of pure TiO₂ spectra coated on glass microspheres and TiO₂-P/SPA is shown in Fig. 6. To estimate the optical band-gap energy of nanostructures, Tauc plot method (Tauc) was used. In this method, the relation known as Kubelka-Munk model is used [33]. These values were calculated to be equal to an energy gap of 3.2 eV for TiO₂ thin film and 2.91 eV for TiO₂-P, respectively. This was in agreement with that obtained by Lin et al. [25]. It can be observed, the effect of the addition of P nonmetal element in the crystalline structure of TiO₂ powder made the gap energy narrower and transferred photocatalytic activity TiO₂-P to the visible region [23,34,35]. It should be noted that the energy gap of TiO₂-P coated on SPA is less than TiO₂-N,S thin film on glass microspheres (2.96 eV) was reported in previous literature [22]. Therefore, we compared the photooxidation property of naphthalene degradation in the presence of TiO₂-P coated on SPA glass microspheres with TiO₂-N,S thin film on glass microspheres in the presence of visible light (to complete the previous study). So TiO₂-P has better photooxidation properties in the degradation of naphthalene than TiO₂-N,S in the presence of visible light.

3.2. Effect of the initial naphthalene concentration on the efficiency of naphthalene removal

Initial naphthalene concentration as the first parameter was studied. These tests were conducted for 150 min

and at five initial concentrations of naphthalene 5, 15, 25, 40, and 50 mg/L at pH 5. Fig. 7 illustrates that naphthalene concentration decreases over time. The highest optical degradation in the presence of visible light for TiO₂-N,S at 60 min (after 40 min of visible light irradiation) and for TiO₂-P at 50 min (after 30 min of visible light irradiation) was obtained at a concentration of 25 mg/L. The generation rate of oxidizing components such as free hydroxyl

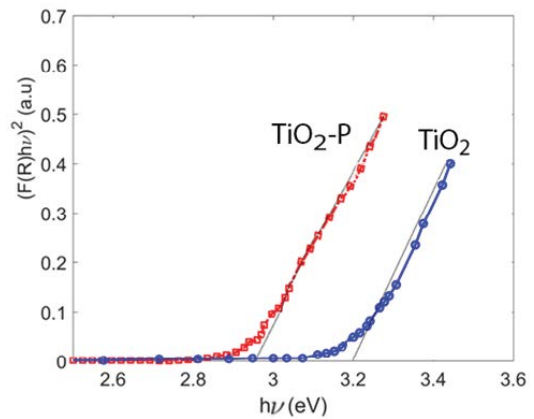


Fig. 6. DRS spectrum of pure TiO₂ coated on glass microspheres (blue line) and TiO₂-P/SPA (red line).

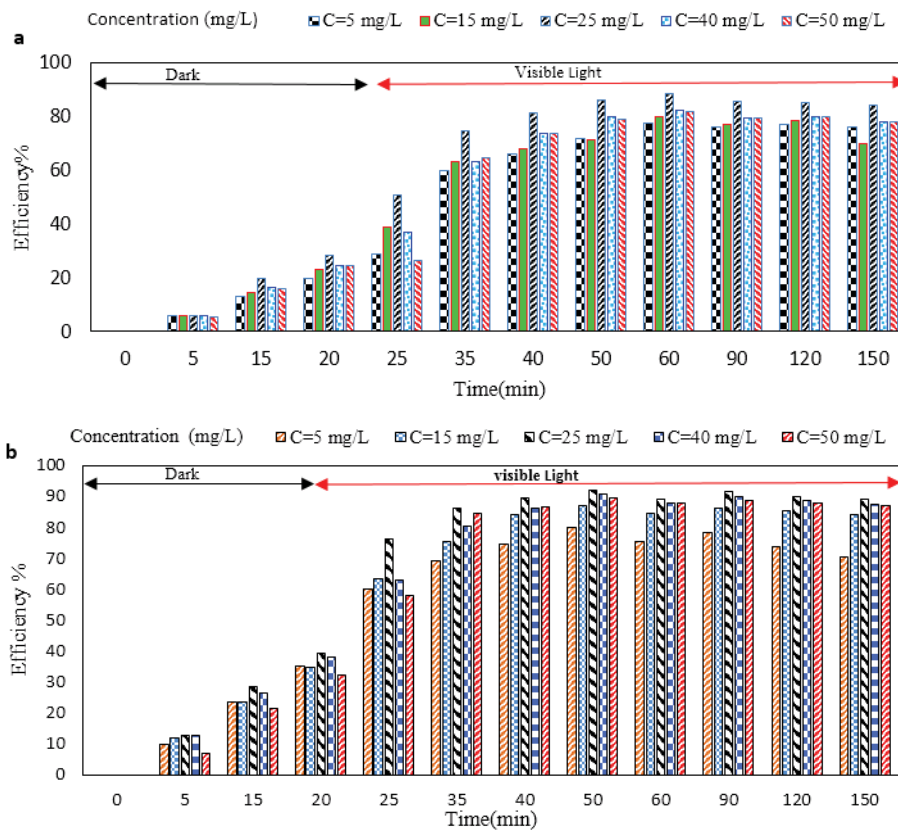


Fig. 7. Efficiency of optical degradation of naphthalene at different initial concentrations in the presence of photocatalyst by: (a) TiO₂-N,S thin film coated on glass microspheres under the dark and visible light conditions from 0 to 150 min and (b) TiO₂-P/SPA under the dark and visible light condition from 0 to 150 min.

radicals was increased under visible light radiation which similar results have been described in previous studies [36].

3.3. Effect of visible light on the efficiency of naphthalene removal

Visible light plays an important role in the process of photocatalytic degradation. This test was done in two stages, that is, darkness and under visible light. The first stage was done in the darkness (at 20 min) and the second stage was done after the first stage (at 130 min) under visible light. Table 1 illustrates the effect of visible light on the degradation rate of naphthalene molecules. Accordingly, when visible light is introduced, the removal of naphthalene was increased because, with the increase of photon count, the formation of electrons and holes has increased, therefore, the share of recombination of holes and electrons is negligible. However, in the dark, the combination of electrons and holes competes with their recombination, reducing the formation of free radicals to accelerate the process of photooxidation in the dark [37]. Removal of naphthalene under the darkness was low. After the first step (for 20 min under dark conditions), the percentage of naphthalene reduction by the $\text{TiO}_2\text{-N,S}$ catalyst is 88.47% after 40 min under visible light radiation, and for the $\text{TiO}_2\text{-P}$ catalyst is 92.12% after 30 min under visible light radiation. The results imply that $\text{TiO}_2\text{-P}$ has better degradation photocatalyst than $\text{TiO}_2\text{-N,S}$ for removal of naphthalene. The photooxidation of naphthalene has been reported in a study with consistent results with our study [17]. According to the titanium sulfide precipitation test (black color) [22], if the Ti^{3+} ion is leached out of catalyst into the solution then it is reacted with the sulfide reagent to the formation of black color precipitated in the vessel. These observations indicated that no leaching of catalyst in aqueous environments.

Table 1

Removal rate of naphthalene by using different catalyst samples: (a) in the darkness for 20 min and (b) under visible light for 130 min ($C = 25 \text{ mg/L}$ and $\text{pH} = 5$)

Time (min) catalyst	Dark condition				Visible light condition							
	0	5	15	20	25	35	40	50	60	90	120	150
$\text{TiO}_2\text{-N,S}$	0	6.06	19.75	28.49	50.54	74.51	81.48	85.89	88.47	85.67	85.25	84.14
$\text{TiO}_2\text{-P}$	0	12.73	28.49	39.18	76.42	86.29	89.42	92.12	89.29	91.61	90.17	89.09

Table 2

Effect of pH on efficiency of naphthalene removal by $\text{TiO}_2\text{-N,S}$, and $\text{TiO}_2\text{-P}$ ($C = 5 \text{ mg/L}$ and $p < 0.05$)

Time (min) pH	0	5	15	20	25	35	40	50	60	90	120	150
	$\text{TiO}_2\text{-N,S}$ 3	0	4.92	10.68	19.45	20.35	44.27	47.12	51.59	56.42	55.20	55
$\text{TiO}_2\text{-P}$	0	7.11	14.84	25.66	42.83	50.10	57.46	59.59	54.26	57.31	55.05	53.08
$\text{TiO}_2\text{-N,S}$ 5	0	5.63	12.86	19.82	28.60	59.78	66.04	71.67	77.32	75.98	76.78	76.15
$\text{TiO}_2\text{-P}$	0	9.65	23.50	35.01	60.19	69.40	74.67	79.96	75.63	78.16	73.68	70.65
$\text{TiO}_2\text{-N,S}$ 7	0	6.95	8.69	17.71	19.34	34.32	45.57	50.57	53.40	51.98	52.61	51.14
$\text{TiO}_2\text{-P}$	0	5.64	15.34	23.84	40.39	46.71	53.50	56.54	51.25	54.17	52.01	50.32
$\text{TiO}_2\text{-N,S}$ 9	0	2.10	2.40	6.24	6.59	21.86	30.01	31.93	32.72	25.79	26.44	24.27
$\text{TiO}_2\text{-P}$	0	1.84	8.51	14.40	23.59	29.22	34.54	37.21	33.59	36.16	34.26	33.09

3.4. Effect of pH on efficiency of naphthalene removal

The effect of pH on the efficiency of naphthalene removal was investigated in the presence of visible light and $\text{TiO}_2\text{-N,S}$, $\text{TiO}_2\text{-P}$ catalysts at pH 3, 5, 7, and 9 at an initial concentration of naphthalene of 5 mg/L. Then, samples were taken at different time intervals (0, 5, 15, 20, 25, 35, 40, 50, 60, 90, 120, and 150 min). Eq. (6) was used to measure naphthalene removal percentage by measuring the optical absorbance of samples at 276 nm.

The pH of the solution has a substantial impact on the process. As a result, the photooxidation degradation rate varies depending on the pH of the aqueous medium which corresponds to the literature reports [22,38,39].

According to Table 2, the maximum removal yield of naphthalene by $\text{TiO}_2\text{-N,S}$ was obtained at pH 5 within 60 min (77.32%), and maximum removal efficiency of naphthalene by $\text{TiO}_2\text{-P}$ was obtained at pH 5 within 50 min (79.96%), which was significantly different from other pHs within 50 and 60 min ($p < 0.05$).

Over time, hydroxyl radicals, which are better formed in an acidic environment, increase the removal efficiency due to the oxidation effect of the creating electron cavity [40–42].

3.5. Chemical oxygen demand

Chemical oxygen demand (COD) test was done according to the Standard Methods for the Examination of Wastewater [31]. The efficiency removal of COD at different time intervals is illustrated in Fig. 8. This observation regarding COD is in line with the above result regarding photodecomposition of naphthalene, that is, the $\text{TiO}_2\text{-P}$ and $\text{TiO}_2\text{-N,S}$ catalysts showed the highest removal efficiency under visible light. The removal of COD in concentration equal 5 mg/L for $\text{TiO}_2\text{-N,S}$ was obtained at 79.26%

and for $\text{TiO}_2\text{-P}$ 81.64%. Therefore, the concentration and pH were the two main factors for COD removal under visible light, so that comparably greater removal rates of COD were observed under alkaline condition (pH = 9).

3.6. Intermediate compounds produced by the degradation of naphthalene

To study the intermediate compounds from the procedure of photooxidation degradation of naphthalene by $\text{TiO}_2\text{-P}$ photocatalyst, gas chromatography (Agilent Technologies 7890A model GC) manufactured by Agilent, USA device connected to mass spectrometer (Agilent Technologies-5975C Model) was used, and the samples were injected into GC-MS after being extracted by dichloromethane solvent. Fig. 9 shows the GC spectrum of the intermediate compounds produced from naphthalene photooxidation by $\text{TiO}_2\text{-P}$ catalyst during irradiation at 0, 35, 55, and 120 min. According to the retention time and evaluation of the device library based on the interpretation of the mass spectrum, the intermediate compounds were determined. It should be noted that in the previous study, the intermediate compounds produced due to naphthalene photooxidation degradation and degradation proposed mechanism for naphthalene removal in the presence of OH radicals were presented [22]. The results are in agreement with the results of previous work. The

intermediate compounds include phthalic acid, 1,2-naphthalene dione, 1,4-naphthalene dione, and 2-carboxy-cinnamaldehyde. The GC-MS results regarding the solution after 120 min confirmed the removal of intermediates.

4. Conclusion

The efficiency of photocatalytic processes for PAH degradation depends not only on the operating conditions

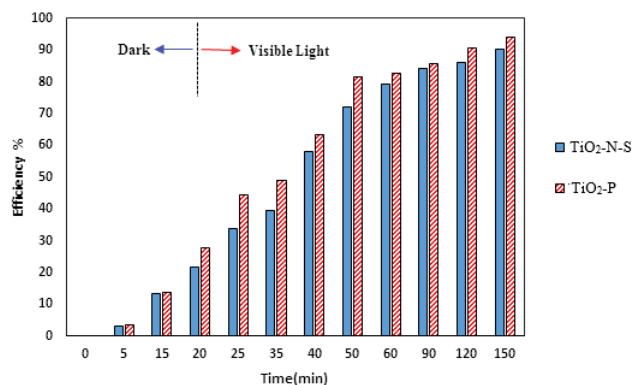


Fig. 8. Efficiency removal of chemical oxygen demand (COD) at different time intervals.

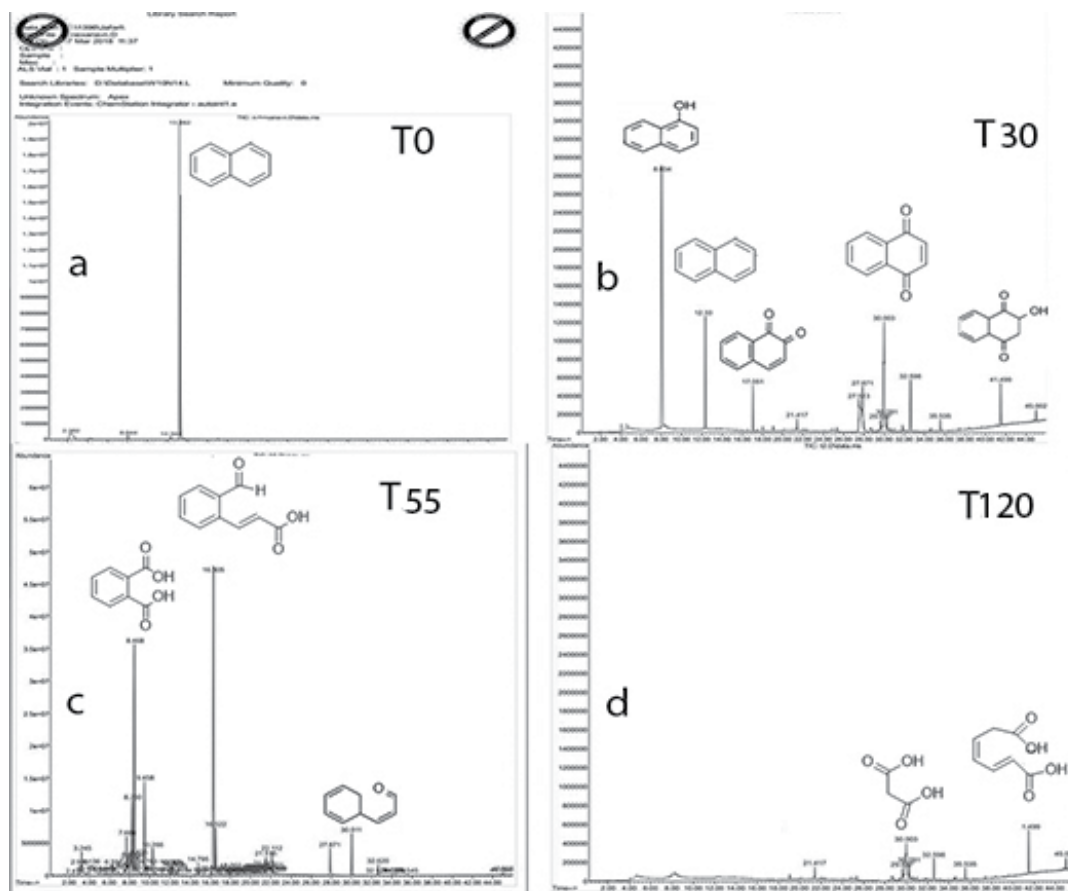


Fig. 9. Intermediate compounds produced from naphthalene photooxidation by $\text{TiO}_2\text{-P}$ catalyst during irradiation at T_0 , T_{30} , T_{55} and T_{120} min.

(e.g., pH, type of energy source, initial pollutant concentration, and reaction time) but also the type of photocatalyst efficiency which determines the quantity of radicals available to oxidize PAHs. The use of photocatalyst will also reduce the likelihood of the occurrence of highly toxic by-products because it can degrade the naphthalene completely into CO₂ and H₂O. In the current study, the novel high-efficiency photocatalyst TiO₂-P immobilized on SPA was prepared by a simple modified sol-gel method. This catalyst was investigated to remove naphthalene from wastewater. DRS analysis showed the energy bandgap narrowing of TiO₂-P convert to the visible region. The excellent photocatalytic activity of TiO₂-P/SPA compared with TiO₂-N-S coated on glass microspheres were studied for removal of naphthalene. By increasing the initial concentration of naphthalene from 5 to 25 mg/L at an exposure time of 60 min, in the presence of visible light, the removal efficiency by TiO₂-N-S catalyst increased from 77.32% to 88.47%, and for TiO₂-P catalyst at 50 min, in the presence of visible light, the removal efficiency increased from 79.96% to 92.12% at pH equal 5. The maximum removal efficiency of naphthalene in the presence of visible light was obtained at a concentration of 25 mg/L. Under acidic conditions and in presence of visible light, TiO₂-N-S and TiO₂-P catalysts were more efficient. The pH and concentration are the two main factors that influence the efficiency of the photocatalysis process. The decomposition of naphthalene was monitored by COD. The removal of COD in pH 5 for TiO₂-N-S was obtained at 79.26% and for TiO₂-P was obtained at 81.64%. GC/MS study results showed that some intermediate compounds are produced and these intermediates are mineralized after another 120 min contact time. It is suggested that the efficiency of TiO₂-P/SPA photocatalysis for removal of the total PAHs.

Acknowledgments

This research has been supported by Islamic Azad University, Tehran Science and Research Branch, Tehran.

References

- [1] S. Fazlollahi, A. Hassani, M. Borghei, H. Pourzamani, Efficiency of multi-walled carbon nanotubes in TPH adsorption in aqueous solution, *J. Environ. Sci. Technol.*, 19 (2017) 132–141.
- [2] X. Zhou, D. Huang, G. Zeng, L. Chen, L. Qin, P. Xu, M. Cheng, C. Huang, C. Zhou, Preparation of water-compatible molecularly imprinted thiol-functionalized activated titanium dioxide: selective adsorption and efficient photodegradation of 2,4-dinitrophenol in aqueous solution, *J. Hazard. Mater.*, 346 (2018) 113–123.
- [3] USEPA, Health Effects Support Document for Naphthalene, Office of Water Health and Ecological Criteria Division, U.S. Environmental Protection Agency, Washington, DC, 2003.
- [4] D. González, L. Ruiz, G. Garralón, F. Plaza, J. Arévalo, J. Parada, B. Moreno, M. Angela-Gomes, Wastewater polycyclic aromatic hydrocarbons removal by membrane bioreactor, *Desal. Water Treat.*, 42 (2012) 94–99.
- [5] I. Manariotis, H. Karapanagioti, C. Chrysikopoulos, Degradation of PAHs by high frequency ultrasound, *Water Res.*, 45 (2011) 2587–2594.
- [6] F. Buseti, A. Heitz, M. Cuomo, S. Badoer, P. Traverso, Determination of sixteen polycyclic aromatic hydrocarbons in aqueous and solid samples from an Italian wastewater treatment plant, *J. Chromatogr. A*, 1102 (2006) 104–115.
- [7] E. Manoli, C. Samara, The removal of polycyclic aromatic hydrocarbons in the wastewater treatment process: experimental calculations and model predictions, *J. Environ. Pollut.*, 151 (2008) 477–485.
- [8] M.J. Garcia-Martinez, L. Canoira, G. Blazquez, I.D. Riva, R. Alcantara, J.F. Llamas, Continuous photodegradation of naphthalene in water catalyzed by TiO₂ supported on glass Raschig rings, *Chem. Eng. J.*, 110 (2005) 123–128.
- [9] L. Antoine, F. Corinne, C. Jean-Marc, H. Jean-Marie, Naphthalene degradation in water by heterogeneous photocatalysis: an investigation of the influence of inorganic anions, *J. Photochem. Photobiol., A*, 193 (2008) 193–203.
- [10] E. Veignie, C. Rafin, D. Landy, S. Fourmentin, G. Surpateanu, Fenton degradation assisted by cyclodextrins of a high molecular weight polycyclic aromatic hydrocarbon benzo[a]pyrene, *J. Hazard. Mater.*, 168 (2009) 1296–1301.
- [11] N. Vela, M. Martínez-Menchón, G. Navarro, G. Pérez-Lucas, S. Navarro, Removal of polycyclic aromatic hydrocarbons (PAHs) from groundwater by heterogeneous photocatalysis under natural sunlight, *J. Photochem. Photobiol., A*, 232 (2012) 32–40.
- [12] M. Pera-Titus, V. Garcia-Molina, M. Banos, J. Giménez, S. Esplugas, Degradation of chlorophenols by means of advanced oxidation processes: a general review, *Appl. Catal., B*, 47 (2004) 219–256.
- [13] W. Qin, J. Qi, Y. Chen, H. Li, X. Wu, Visible light derived N,S-codoped TiO₂ photocatalysts grown by microplasma oxidation method, *J. Electrochem. Sci.*, 8 (2013) 7680–7686.
- [14] S. Nandy, A. Banerjee, E. Fortunato, R. Martins, A review on Cu₂O and Cu based p-type semiconducting transparent oxide materials, *Rev. Adv. Sci. Eng.*, 2 (2013) 273–304.
- [15] S. Murgolo, F. Petronella, R. Ciannarella, R. Comparelli, A. Agostiano, M.L. Curri, G. Mascolo, UV and solar-based photocatalytic degradation of organic pollutants by nano-sized TiO₂ grown on carbon nanotubes, *Catal. Today*, 240 (2015) 114–124.
- [16] B. Latkovaska, J. Figa, Cyanide removal from industrial wastewater, *Pol. J. Environ. Study*, 16 (2007) 748–752.
- [17] B. Wang, G. Zhang, X. Leng, Z. Sun, S. Zheng, Characterization and improved solar light activity of vanadium doped TiO₂/diatomite hybrid catalysts, *J. Hazard. Mater.*, 285 (2015) 212–220.
- [18] J. Fan, Z. Zhao, W. Liu, Y. Xue, S. Yin, Solvothermal synthesis of different phase N-TiO₂ and their kinetics, isotherm and thermodynamic studies on the adsorption of methyl orange, *J. Colloid Interface Sci.*, 470 (2016) 229–236.
- [19] X.F. Lei, X.X. Xue, H. Yang, C. Chen, X. Li, J.X. Pei, M.C. Niu, Y.T. Yang, X.Y. Gao, Visible light-responded C, N and S co-doped anatase TiO₂ for photocatalytic reduction of Cr(VI), *J. Alloys Compd.*, 646 (2015) 541–549.
- [20] A. Khalilzadeh, S. Fatemi, Modification of nano-TiO₂ by doping with nitrogen and fluorine and study acetaldehyde removal under visible light irradiation, *Clean Technol. Environ. Policy*, 16 (2014) 629–636.
- [21] R. Fagan, D.E. McCormack, S. Hinder, S.C. Pillai, Improved high temperature stability of anatase TiO₂ photocatalysts by N, F, P co-doping, *Mater. Des.*, 96 (2016) 44–53.
- [22] A. Jafari, M. Sadeghi, F. Tirgir, S.M. Borghaei, Sulfur and nitrogen doped-titanium dioxide coated on glass microspheres as a high performance catalyst for removal of naphthalene (C₁₀H₈) from aqueous environments using photo oxidation in the presence of visible and sunlight, *Desal. Water Treat.*, 192 (2020) 195–212.
- [23] M. Iwase, K. Yamada, T. Kurisaki, O.O. Prieto-Mahaney, B. Ohtani, H. Wakit, Visible-light photocatalysis with phosphorus-doped titanium(IV) oxide particles prepared using a phosphide compound, *Appl. Catal., B*, 132–133 (2013) 39–44.
- [24] L. Korosi, I. Dekany, Preparation and investigation of structural and photocatalytic properties of phosphate modified titanium dioxide, *Colloids Surf., A*, 280 (2006) 146–154.
- [25] L. Lin, W. Lin, Y. Zhu, B. Zhao, Y. Xie, Phosphor-doped titania a novel photocatalyst active in visible light, *Chem. Lett.*, 34 (2005) 284–285.

- [26] A. Bamoniri, B.F. Mirjalili, S. Nazemian, Nano silica phosphoric acid: an efficient catalyst for the one-pot synthesis of amidoalkyl naphthols under solvent-free condition, *J. Iran.Chem. Soc.*, 11 (2014) 653–658.
- [27] R. Zheng, L. Line, J. Xie, Y. Zhu, Y. Xie, State of doped phosphorus and its influence on the physicochemical and photocatalytic properties of P-doped titania, *J. Phys. Chem. C*, 112 (2008) 15502–15509.
- [28] L. Lin, W. Lin, J.L. Xie, Y.X. Zhu, B.Y. Zhao, Y.C. Xie, Photocatalytic properties of phosphor-doped titania nanoparticles, *Appl. Catal. B*, 75 (2007) 52–58.
- [29] F. Mohamadi-Moghadam, M. Sadeghi, N. Masoudipour, Degradation of cyanide using stabilized TiO₂-S,N nanoparticles by visible and sun light, *J. Adv. Oxid. Technol.*, 21 (2018) 274–284.
- [30] V. Mahmoodi, J. Sargolzae, Photocatalytic abatement of naphthalene catalyzed by nanosized TiO₂ particles: assessment of operational parameters, *Theor. Found. Chem. Eng.*, 48 (2014) 656–666.
- [31] E.W. Rice, R.B. Baird, A.D. Eaton, L.S. Clesceri, *Standard Methods for the Examination of Water and Wastewater*, American Public Health Association, Washington, DC, 2005.
- [32] L.Yingying, Y.b. Leshu, H. Heyong, L. Hailong, F. Yuying, Preparation, characterization of P-doped TiO₂ nanoparticles and their excellent photocatalytic properties under the solar light irradiation, *J. Alloys Compd.*, 488 (2009) 314–319.
- [33] R. Lopez, R. Gomez, Band-gap energy estimation from diffuse reflectance measurements on sol-gel and commercial TiO₂: a comparative study, *J. Sol-Gel. Sci. Technol.*, 61 (2012) 1–7.
- [34] F. Li, Y. Jiang, M. Xia, M. Sun, B. Xue, D. Lin, X. Zhang, Effect of the P/Ti ratio on the visible-light photocatalytic activity of P-doped TiO₂, *J. Phys. Chem. C*, 113 (2009) 18134–18141.
- [35] K. Yang, Y. Dai, B. Huang, Understanding photocatalytic activity of S- and P-doped TiO₂ under visible light from first-principles, *J. Phys. Chem. C*, 111 (2007) 18985–18994.
- [36] Y.G. Montaser, S.J. Tarek, E.S. Ibrahim, R.S. Eglal, A.N. Rabab, Treatment of highly polluted paper mill wastewater by solar photocatalytic oxidation with synthesized nano TiO₂, *Chem. Eng. J.*, 168 (2011) 446–454.
- [37] D. Dong, P. Li, L. Xiaojun, Q. Zhao, Y. Zhang, C. Jia, P. Li, Investigation on the photocatalytic degradation of pyrene on soil surfaces using nanometer anatase TiO₂ under UV irradiation, *J. Hazard. Mater.*, 174 (2009) 859–863.
- [38] A. Durán, J.M. Monteagudo, Solar photocatalytic degradation of reactive blue 4 using a Fresnel lens, *Water Res.*, 41 (2006) 690–698.
- [39] A. Lin, J.H. Hsueh, P. Hong, Removal of antineoplastic drugs cyclophosphamide, ifosfamide, and 5-fluorouracil and a vasodilator drug pentoxifylline from wastewaters by ozonation, *Environ. Sci. Pollut. Res. Int.*, 22 (2014) 508–515.
- [40] D. Avisar, Y. Lester, H. Mamane, pH induced polychromatic UV treatment for the removal of a mixture of SMX, OTC and CIP from water, *J. Hazard. Mater.*, 175 (2010) 1068–1074.
- [41] J. Pettibone, D. Cwiertny, M. Scherer, V. Grassian, Adsorption of organic acids on TiO₂ nanoparticles: effects of pH, nanoparticle size, and nanoparticle aggregation, *Langmuir*, 24 (2008) 6659–6667.
- [42] A.G. Rincón, C. Pulgarin, Effect of pH, inorganic ions, organic matter and H₂O₂ on *E. coli* K12 photocatalytic inactivation by TiO₂: implications in solar water disinfection, *Appl. Catal., B*, 51 (2004) 283–302.